

Supporting information

A new chiral Fe(III)-salen grafted mesoporous catalyst for enantioselective asymmetric ring opening of racemic epoxides at room temperature under solvent-free conditions

Susmita Roy^{†,a}, Piyali Bhanja^{†,b}, Sk. Safikul Islam,^a Asim Bhaumik^{b*} and Sk. Manirul Islam^{a*}

^aDepartment of Chemistry, Kalyani University, Kalyani, Nadia, India

^bDepartment of Materials Science, Indian Association for the Cultivation of Science, Jadavpur 700 032, India

[†]these authors contributed equally

Table of Contents

Section-S1	Details of chemicals used, equipments employed, experimental procedure for the synthesis of Fe@SBSAL and experimental for the catalytic asymmetric ring opening (ARO) reaction of epoxides.
Table S1	Optimization of the reaction conditions over Fe@SBSAL
Table S2	Comparison of catalytic activity of the Fe@SBSAL catalyst with respect to other related reported systems.
Table S3	Comparison of catalytic activity between homogeneous Fe(III) salen complex and heterogeneous chiral catalyst (Fe@SBSAL) in the ARO reaction.
Figure S1	FT IR spectrum of Fe@SBSAL.
Figure S2	¹ H NMR of chiral salen ligand (3).
Figure S3	HRMS of homogeneous chiral Fe(III)-salen complex (4).
Figure S4	The small angle powder X-ray diffraction pattern of (a) pure SBA-15 and (b) AM-SBA-15 materials.
Figure S5	The nitrogen adsorption/desorption isotherm of pure SBA-15 (a) and AM-SBA-15 (b) materials.
Figure S6	NLDFT pore size distributions corresponding to the N ₂ adsorption isotherms of pure SBA-15 (a) and AM-SBA-15 (b) materials.
Figure S7	Thermal analysis of the Fe@SBSAL material.
Figure S8	The DRS-UV-visible absorption spectrum of Fe@SBSAL material.

Figure S9	EPR spectrum of fresh Fe@SBSAL catalyst.
Figure S10	Recyclability of Fe@SBSAL in the ARO reaction.
Figure S11	The XPS spectrum of reused Fe@SBSAL catalyst.
Section-S2	¹ H NMR and HPLC data of isolated pure products.
Section-S3	¹ H NMR spectra and HPLC data.
Section-S4	References

Section-S1

Chemicals

Pluronic P123 (EO₂₀PO₇₀EO₂₀, EO = ethylene oxide, PO = propyleneoxide, M_{av} = 5800), Tetraethoxysilicate (TEOS), 3-aminopropyl triethoxysilane (3-APTES), (1*S*,2*S*)-(+)-1,2-diaminocyclohexane, 3-*tert*-Butyl-2-hydroxybenzaldehyde and all racemic epoxides were purchased from Aldrich Chemical Co. FeCl₃·6H₂O and all anilines were purchased from E-Merck. All the reagents were analytical grade and used as such without further purification. Solvents were purified and dried according to standard procedures. Thin layer chromatography was done using commercial (MERCK) plates with silica gel 60 F₂₅₄.

Characterizations

Powder X-ray diffraction (PXRD) patterns of different samples were recorded with a Bruker D8 Advance X-ray diffractometer operated at a voltage of 40 kV and a current of 40 mA using Ni-filtered Cu K α ($\lambda=0.15406$ nm) radiation. UV-visible diffuse reflectance spectra were recorded on a Shimadzu UV 2401PC coupled with an integrating sphere attachment. BaSO₄ was used as background standard. Thermogravimetric analysis (TGA) was carried out using a Mettler Toledo TGA/DTA 851e. Transmission electron microscopy (TEM) images of the mesoporous mixed oxide were obtained using a JEOL JEM 2010 transmission electron microscope with operating voltage 200 kV. The samples were prepared by dropping a colloidal solution onto the carbon-coated copper grids followed by drying under high vacuum. For the bulk elemental analysis the Fe@SBSAL was digested with acid to dissolved them into clear liquid and then Fe content were analyzed by using a Shimadzu AA-6300 atomic absorption spectrophotometer (AAS) fitted with a double beam monochromator. Carbon, hydrogen and nitrogen contents of Fe@SBSAL was analyzed using a Perkin Elmer

2400 Series II CHN analyzer. Nitrogen sorption isotherms were obtained using a Quantachrome Autosorb 1C surface area analyzer at 77 K. Prior to the measurement, the samples were degassed at 423 K for approximately 4 h under high vacuum. ^1H NMR spectra were recorded on a Bruker DPX-400 instruments. The FT-IR spectra of the samples were recorded on a Perkin-Elmer FT-IR 783 spectrophotometer. Enantiomeric excesses (ee) were determined by HPLC (Agilent, Model 1220) using Ultron using a Chiralcel ® OD-H column (wavelengths 254 nm) with 2-propanol/hexane as eluent. Optical rotations are reported as follows: $[\alpha]_{\text{D}}^{27}$ (c = in g per 100 ml, solvent) were measured with a Digipol 781 Automatic Polarimeter Rudolph Instruments.

1. Experimental procedure for synthesis of Fe@SBSAL catalyst

1.1 Synthesis of the homogeneous chiral Fe(III) salen complex **4**

The homogeneous chiral Fe (III) salen complex (Fe-SAL) **4** was prepared as follows.

1.1.1. Synthesis of 3-tert-butyl-5-chloromethyl-2-hydroxybenzaldehyde¹ (**2**)

At first, 3-tert-Butyl-2-hydroxybenzaldehyde (2.7 g, 15.2 mmol) was reacted with paraformaldehyde (1.0 g, 33.3 mmol) in 11 ml of concentrated hydrochloric acid under vigorous stirring for 72 h at 313 K¹. Then the reaction mixture was repeatedly extracted with diethyl ether (3×15 ml), washed with 5% NaHCO_3 (2×10 ml) and brine (2×10 ml). The organic layer were dried over anhydrous Na_2SO_4 and evaporated to obtain **2** as a yellow crystalline solid (3.0 g, 90% yield). ^1H NMR (CDCl_3 , 400 MHz): δ (ppm) 1.46 (s, 9H), 4.67 (s, 2H), 7.42 (d, J = 2.4 Hz, 1H), 7.52 (d, J = 2 Hz, 1H), 9.88 (s, 1H), 11.78 (s, 1H).

1.1.2. Synthesis of chiral ligand² (**3**)

In this procedure², 2.7 g of 3-tert-butyl-5-chloromethyl-2-hydroxybenzaldehyde (**2**) was transferred to a Schlenk flask filled with 0.7 g of (1*S*,2*S*)-(+)-1,2-diaminocyclohexane (6 mmol). The mixture was dissolved under stirring condition in 45 ml absolute ethanol and refluxed for 3 h. The resulting reaction mixture was cooled to room temperature, and 14 ml of deionized water was added. The mixture was kept at 0-5 °C in the refrigerator overnight; then the yellow precipitated ligand (92% yield) was filtered and washed with 5 ml ethanol. ^1H NMR ($\text{DMSO-}d_6$, 400 MHz): δ (ppm) 1.30 (s, 18H), 1.33–1.99 (m, 8H), 3.35–3.45 (m, 2H), 4.31 (s, 4H), 7.05 (m, 2H), 7.18–7.20 (m, 2H), 8.46 (s, 2H), 14.06 (bs, 2H).

1.1.3. Synthesis of homogeneous chiral Fe(III) salen complex 4

Chiral ligand **3** (5 mmol) was added to a solution of FeCl₃·6H₂O (15 mmol) in absolute ethanol (80 ml). The resulting mixture was refluxed for 8 h. The solvent was completely evaporated under reduced pressure on a rotary evaporator, and the residue was extracted with 80 ml of dichloromethane. The organic phase was washed with deionized water (3 × 25 ml) and brine (2 × 20 ml), and then dried over NaSO₄. This was further concentrated to remove the solvent, and the residue was recrystallized from dichloromethane/hexane to give **4** as a brown solid. TOF-MS *m/z*: calcd (C₃₀H₄₀N₂O₃FeCl₃) 604.17 (M⁺, -Cl), found 604.30 (M⁺, -Cl). FT-IR (KBr): 3185, 2957, 2923, 2853, 1645, 1614, 1542, 1464, 1437, 1310, 1261, 1092, 1025, 934, 865, 810, 721, 653, 546 cm⁻¹.

1.2 Synthesis of mesoporous support

1.2.1 Synthesis of mesoporous SBA-15 material

Mesoporous SBA-15 was synthesized according to the reported procedure³. P123 (4 gm), 2.0(M) aq. HCl (120 mL) and distilled water (15 mL) were mixed at room temperature for 4 h. Then TEOS (8.5 gm) was added drop wise to the solution of P123 at 40 °C for 24 h. After that, a synthesized gel was thus formed, which was then loaded in a 500 mL scaled polypropylene bottle using Teflon tape and was kept at 100 °C for 24 h under static condition. Solid white product was separated by filtration, washed with distilled water, dried in air. Then the product was calcined at 500 °C for 5 h.

1.2.2. Synthesis of 3-amino propyl functionalized SBA-15 (5)

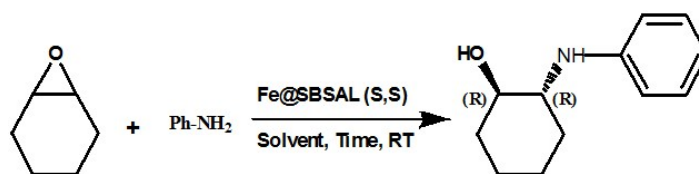
The calcined SBA-15 (2 gm) was refluxed with 3-aminopropyltriethoxysilane (3-APTES) (3.6 gm) in toluene for 18 h.³ The resulting white solid was filtered, washed thoroughly with ethanol and finally dried in air.

1.3. Synthesis of heterogeneous chiral Fe(III) complex (Fe@SBSAL) (6)

The amine-functionalized support of **5** (0.5 g) was added to a solution of complex **4** (0.2 g) in toluene (30 ml). The mixture was refluxed with vigorous stirring for 24 h (Figure 1). The brown solids **6** were collected by filtration, washed with diethyl ether, and then Soxhlet-extracted with dichloromethane for 24 h. The loading of complex **6** in the heterogenized catalyst, based on Fe content, was determined by AAS. FT-IR (KBr): 3413, 3049, 1622, 1467, 1075, 773, 696, 572, 471 cm⁻¹; CHN analysis: C = 11.87 %, H = 2.68 %, N = 2.67 %.

Experimental procedure for asymmetric ring opening (ARO) of epoxides:

In a typical procedure, a mixture comprising of a chiral catalyst Fe@SBSAL (20 mg), an epoxide (1 mmol) and an amine (1 mmol) were taken in a 5 mL round bottom flask and stirred vigorously for a given time period (monitored by TLC) under solvent free condition. The contents were dissolved in 15 mL of chloroform and filtered to recover the catalyst. The catalyst after washing with chloroform thrice (10 mL each) was reactivated in an air oven at 60 °C and reused five times without any loss in its activity and enantioselectivity. The chloroform layer was transferred to a separating funnel and washed twice with water. This was followed by a wash with a saturated solution of sodium chloride. The organic layer was then dried with anhydrous sodium sulfate. The crude product of β -aminoalcohol was then purified by flash column chromatography (mixture of ethyl acetate and hexane) to obtain the corresponding pure product as a single isomer. All compounds were characterized on the basis of their spectroscopic data (¹H NMR) and by comparison with those reported in the literature. Enantiomeric excess (ee) was determined by HPLC analysis using Chiralpak OD column.

Table S1. Optimization of the reaction conditions over Fe@SBSAL^a

Entry	Catalyst Amount (mg)	Solvent	Time (h)	Yield ^b (%)	ee ^c (%)
1.	None	None	24	Trace	nd
2.	30	DCM	4	75	71
3.	30	Toluene	4	69	69
4.	30	H ₂ O	4	81	89
5.	30	None	4	96	99
6.	20	None	4	96	99
7.	20	None	3	96	99
8.	20	None	2	96	99
9.	10	None	2	83	99
10.	20	None	1	81	97

^aReaction conditions: cyclohexene oxide (1 mmol), Aniline(1 mmol), Fe@SBSAL (20 mg, 0.4 mo% of Fe), without solvent, RT;

^bYields refer to those of isolated pure products.

^cenantiomeric excess was determined by HPLC analysis using Chiralpak OD column

Table S2. Comparison of catalytic activity of the present catalyst with respect to other related reported systems

Catalyst	Reaction Condition	Yield ^a (%)	ee ^b (%)	TOF (h ⁻¹)	References
Macrocyclic Chiral Cr(III) salen complex	Catalyst (0.5 mol%), Cyclohexene oxide (1 mmol), anilines (1 mmol) in DCM+MeOH, 24 h, rt.	98	75	8.16	4
Chiral organocatalyst	Catalyst(20mol%),Cyclohexene oxide (0.2 mmol), anilines (0.22 mmol) in DCM, 24 h, rt.	95	89	.04	5
Homogeneous chiral Vanadium–Salan Complex	Catalyst (10mol%), Cyclohexene oxide (1.0 mmol), anilines (1.0 mmol) in DCM, 24 h, 0 °C.	84	62	0.35	6
Heterogeneous chiral Fe(III) salen complex (Fe@SBSAL)	Cyclohexene oxide (1 mmol), Aniline (1 mmol), Fe@SBSAL (0.4 mo% of Fe), without solvent, RT, 2 h.	96	99	121	Present study

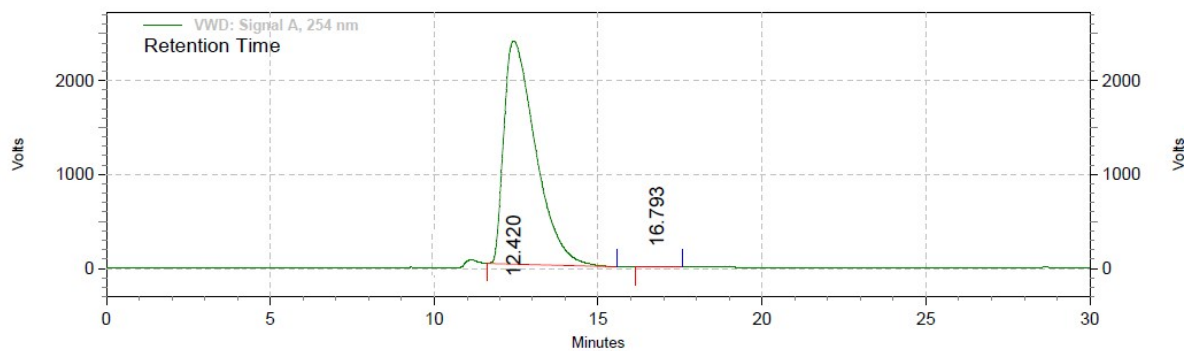
^aYields refer to those of isolated pure products, ^benantiomeric excess was determined by HPLC analysis using Chiralpak OD column.

Table S3. Comparison of catalytic activity between allyl glycidyl ether and aniline catalyzed by homogeneous Fe(III) salen complex (4) and heterogeneous chiral catalyst (Fe@SBSAL)^a for the ARO reaction

Catalyst	Time (h)	Yield ^b (%)	ee ^c (%)	TOF (h ⁻¹)
Homogeneous Fe(III) salen complex	1	96	>99	247
Heterogeneous chiral Fe@SBSAL catalyt	1.5	96	>97	160

^aReaction conditions: Allyl Glycidyl ether (1 mmol), Aniline(1 mmol), Fe@SBSAL (20 mg, 0.4 mo% of Fe), without solvent, RT, ^bYields refer to those of isolated pure products, ^cenantiomeric excess was determined by HPLC analysis using Chiralpak OD column.

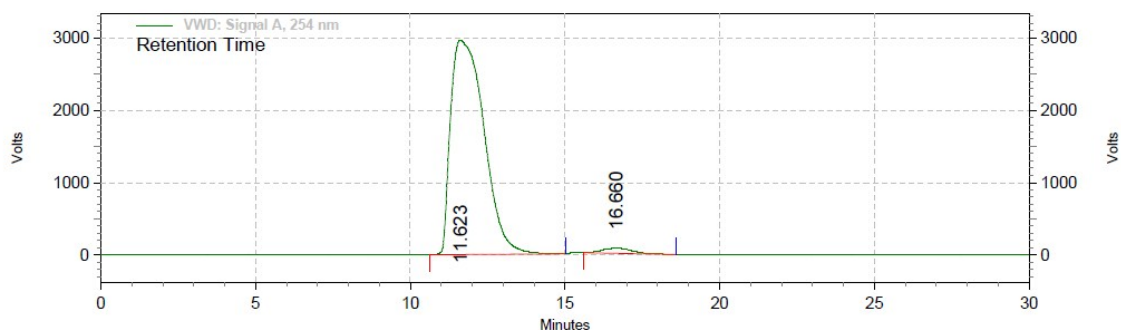
HPLC data of (R)-1-(allyloxy)-3-(phenylamino)propan-2-ol (Synthesized by homogeneous chiral Fe(III) salen complex)



**VWD: Signal A,
254 nm Results**

Retention Time	Area	Area %	Height	Height %
12.420	2671590321	99.93	39874020	99.90
16.793	1951710	0.07	41362	0.10
Totals				
	2673542031	100.00	39915382	100.00

HPLC data of (R)-1-(allyloxy)-3-(phenylamino)propan-2-ol (Synthesized by heterogeneous chiral Fe(III) salen complex)



VWD: Signal A,
254 nm Results

Retention Time	Area	Area %	Height	Height %
11.623	3733007931	97.98	49667254	97.74
16.660	77030307	2.02	1146876	2.26
Totals	3810038238	100.00	50814130	100.00

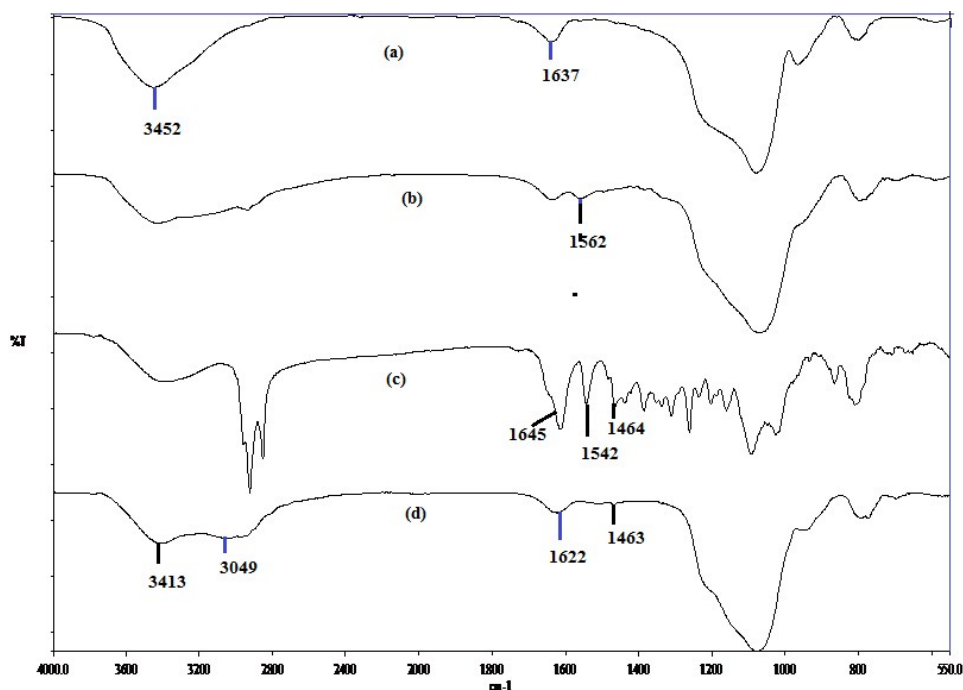


Figure S1. FT IR spectra of SBA-15 (a) 3-aminopropyltriethoxysilane-modified mesoporous silica AM-SBA-15 (b), homogeneous Fe(III)-salen complex (Fe-SAL) (c) and heterogeneous chiral catalyst Fe@SBSAL (d).

Fig. S1 (a-d), represents the FT- IR spectra of the calcined SBA-15, 3 aminopropyltriethoxy silane-modified support (AM-SBA-15), the homogeneous Fe(III)-salen complex(Fe-SAL) and the heterogeneous catalyst Fe@SBSAL. The peaks near 3000 cm^{-1} indicate the C–H stretching vibrations of alkyl groups and the intensity of this peak gradually increases with the modification of 3-aminopropyltriethoxysilane and the immobilization of chiral Fe(III) salen complex (Figure. S1 (b) and (d)). In the FT IR spectrum of AM-SBA-15, band at 1562 cm^{-1} could be assigned to N–H deformation vibrations of amido groups. In Fe-SAL (Figure S1(c)) characteristic IR bands appears at 1645, 1542, and 1464 cm^{-1} , which are due to the stretching vibrations of -C=N groups and the deformation vibrations of C–H bond, respectively. These bands are also present in the heterogeneous catalyst Fe@SBSAL (4). The FT IR spectra confirmed the successful modification of the mesoporous SBA-15 support with 3-aminopropyltriethoxysilane and immobilization of chiral Fe(III) salen complex 4.

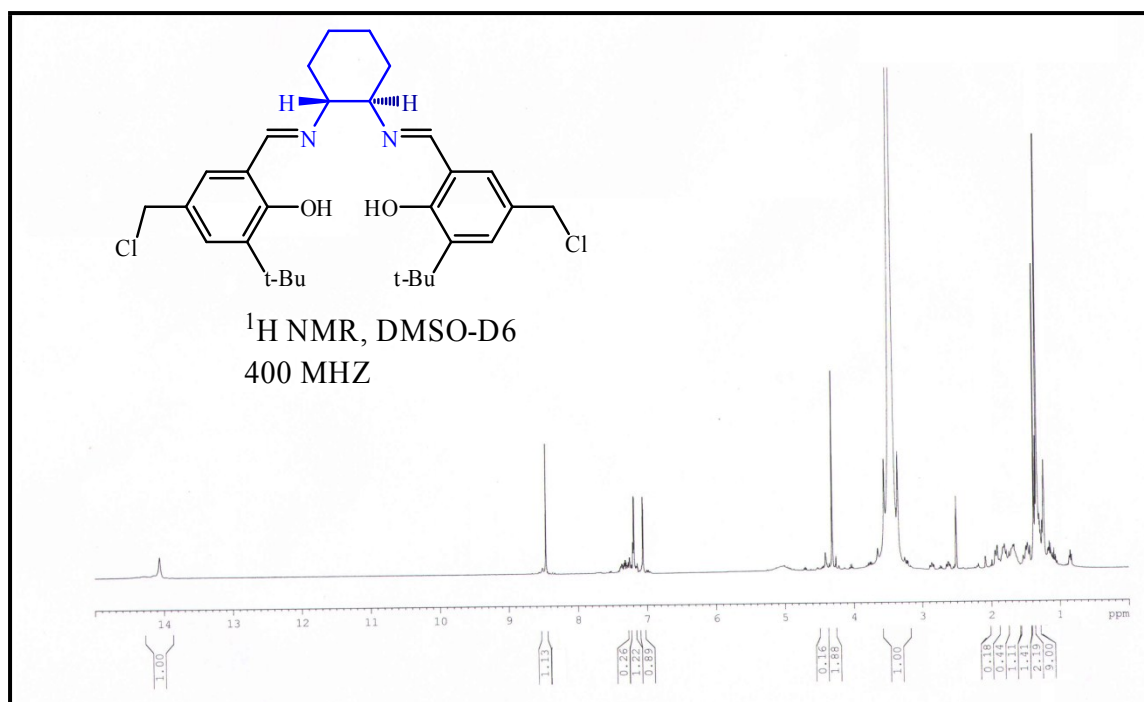


Figure S2. ^1H NMR of chiral salen ligand (**3**)

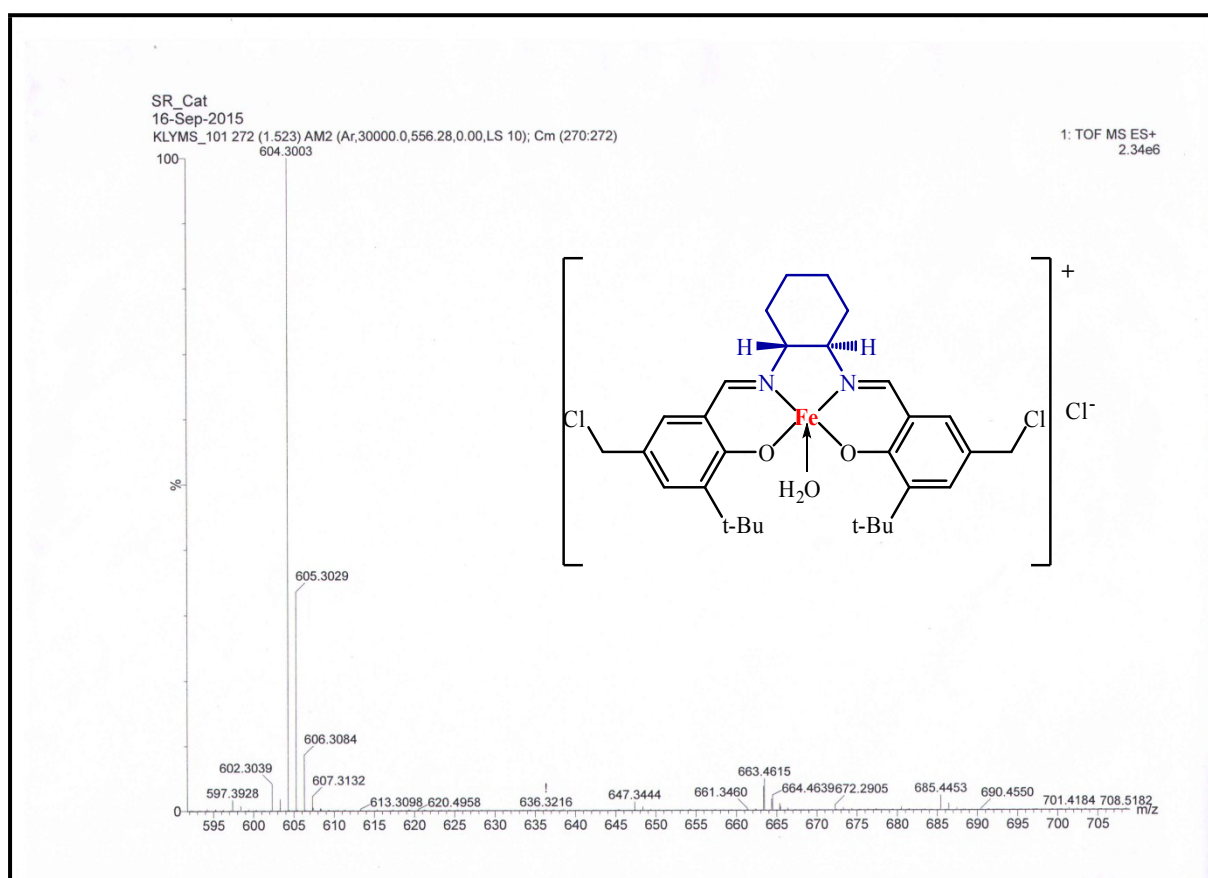


Figure S3. HRMS of homogeneous chiral Fe(III) salen complex (**4**)

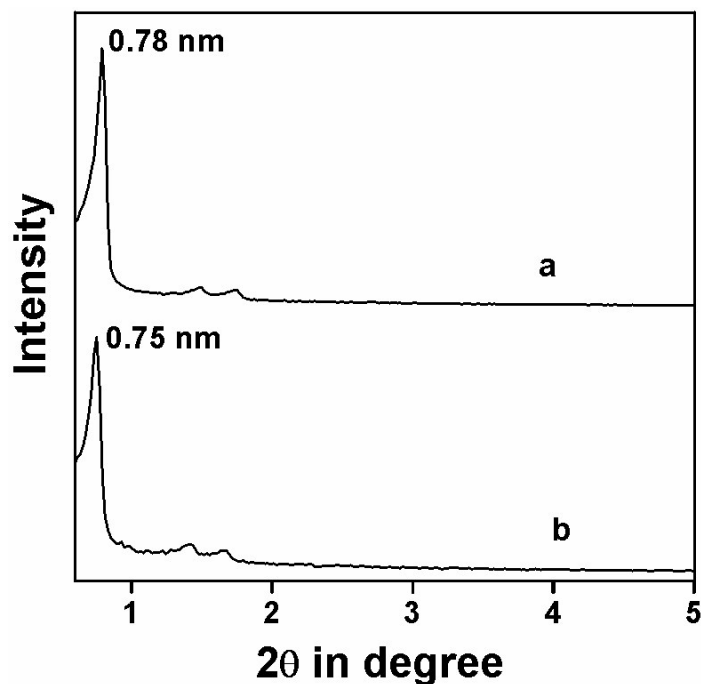


Figure S4. The small angle powder X-ray diffraction pattern of (a) pure SBA-15 and (b) AM-SBA-15 material.

The small angle powder X-ray diffraction patterns of pure silica SBA-15 and 3-aminopropyl functionalized material AM-SBA-15 are shown in Figure S1. As seen from the figure, these two materials exhibited three characteristic peaks corresponding to three distinct planes of 2D-hexagonal mesophase of SBA-15 *i.e.* 100 (strong), 110 (weak), 200 (weak). Little shift in the peak positions toward higher 2θ values (for 100: $0.75 < 0.78 < 0.80$) indicated that successive functionalizations of the pure SBA-15 with 3-aminopropyl followed by the chiral Fe(III) complex. Successive functionalization caused decrease in d -spacings.⁷ This result also suggested that proper functionalization has been occurred at the pore surface of SBA-15 material through this post synthetic pathway.

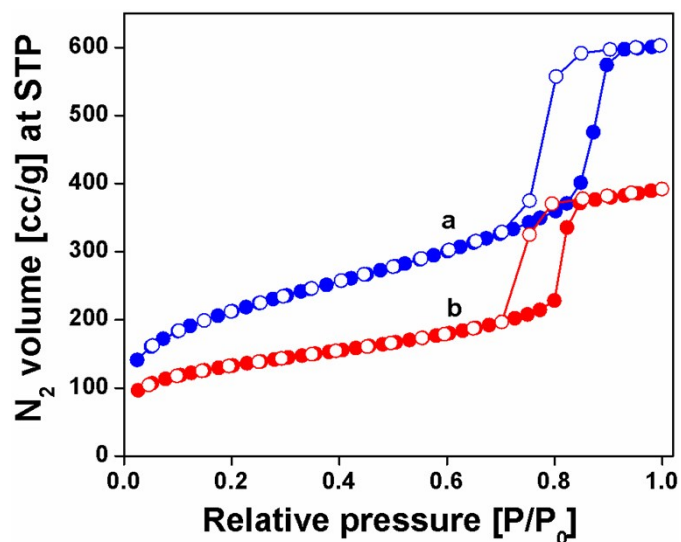


Figure S5. The nitrogen adsorption/desorption isotherm of (a) pure SBA-15 and (b) AM-SBA-15 materials.

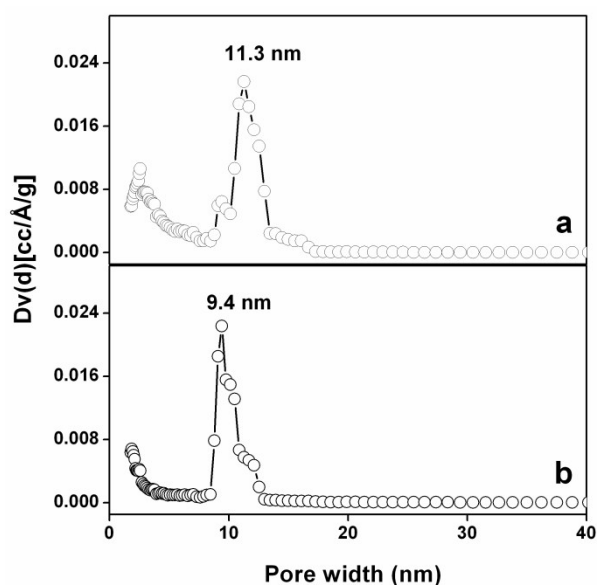


Figure S6. NLDFT pore size distributions corresponding to the N_2 adsorption isotherms of pure SBA-15 (a) and AM-SBA-15 (b) materials.

The nitrogen adsorption/desorption isotherm of pure SBA-15 and AM-SBA-15 have been demonstrated in Figure S2. From the figure it is noticed that both samples displayed typical type IV isotherm with large H1 type hysteresis loop. For SBA-15 and AM-SBA-15 material the hysteresis loops are observed in the high pressure region of 0.71 to 0.92 and 0.70

to 0.85 relative pressure of nitrogen, respectively whereas for Fe@SBSAL material the H1 hysteresis loop is appeared from 0.65 to 0.83 pressure range, suggesting the proper stepwise functionalization of the mesopore surface.⁷ By employing the NLDFT theory the pore size distribution plot has been obtained and this is shown in Figure S3. From the figure, it is observed that the pore diameter of the material is decreasing in the following order: SBA-15 > AM-SBA-15 > Fe@SBSAL, which also indicated the successive grafting of organic functional group as well as iron on to the SBA-15 surface. The pore volume of SBA-15 and AM-SBA-15 materials is found to be 0.9048 and 0.5864 ccg⁻¹, respectively.

Thermal analysis: The quantitative determination of the organic content and the framework stability of the chiral Fe@SBSAL sample are obtained from the thermogravimetric analysis (TGA) under N₂ flow. TGA curve of Fe@SBSAL material is shown in Figure S7. The TGA of this material showed the first weight loss below 100 °C due to desorption of absorbed water. This was followed by a gradual decrease in the weight after 518 °C. Thus this thermal analysis data suggested that Fe@SBSAL sample is stable up to 518 °C (Figure S7).

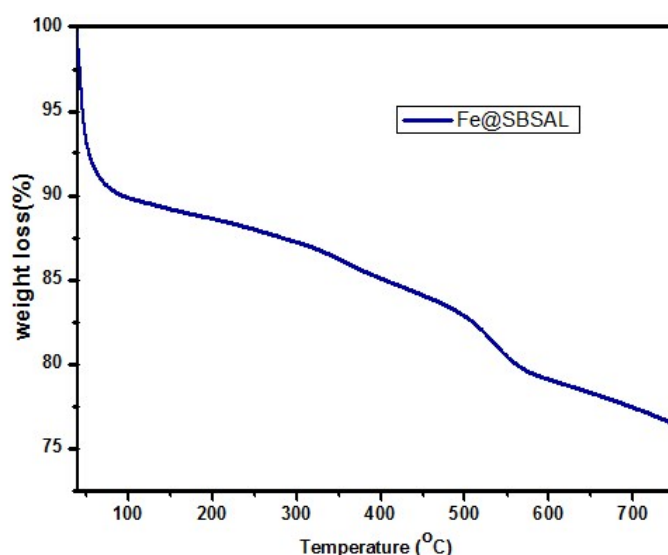


Figure S7. The TGA plot of the Fe@SBSAL material

UV-Vis DRS analysis: The UV–vis absorption spectrum of the Fe@SBSAL is recorded in diffuse reflectance mode as a BaSO₄ disk due to its solubility limitations in common organic solvents. The UV spectra of Fe@SBSAL is given in Figure S8. In this case the vibrational bands at 200-300nm and 326 nm could be attributed due to the n- π^* transitions and the ligand $\pi \rightarrow \pi^*$ transition of phenolic group and azoic group(C=N) respectively. The bands at 350-450 nm was observed arising from metal-to-ligand charge transfer, originated from $d_z^2 \rightarrow \pi^*$, $d_{xz}, d_{yz} \rightarrow \pi^*$ and $d_{xy} \rightarrow \pi^*$.

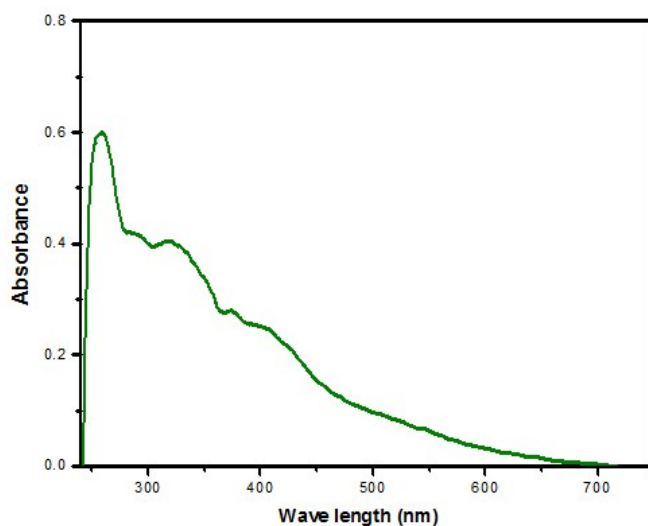


Figure S8. The DRS-UV-visible absorption spectrum of Fe@SBSAL material

Electron paramagnetic resonance spectroscopy (EPR)

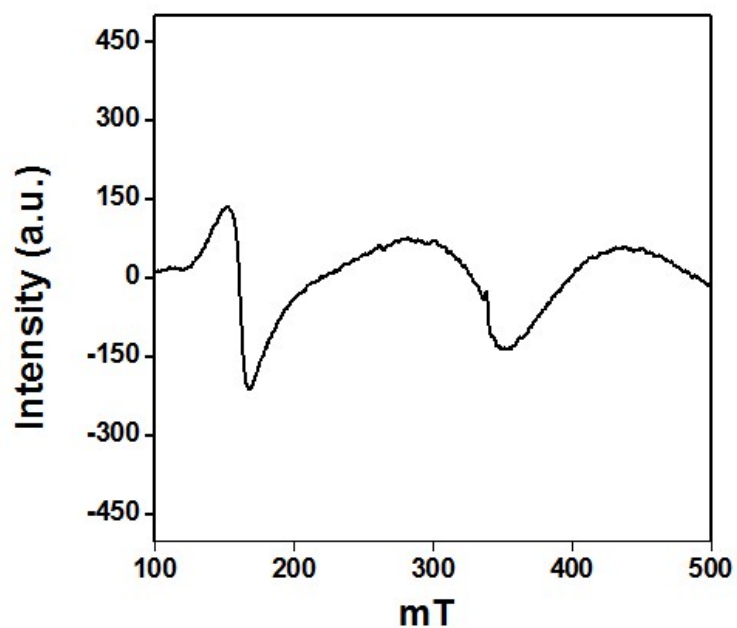


Figure S9. EPR spectrum of fresh Fe@SBSAL catalyst.

Recyclability chart

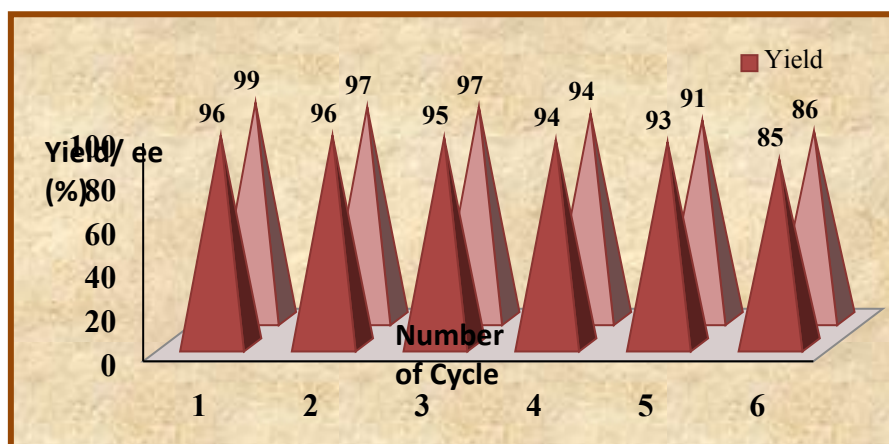


Figure S10. Recyclability of chiral Fe@SBSAL catalyst.

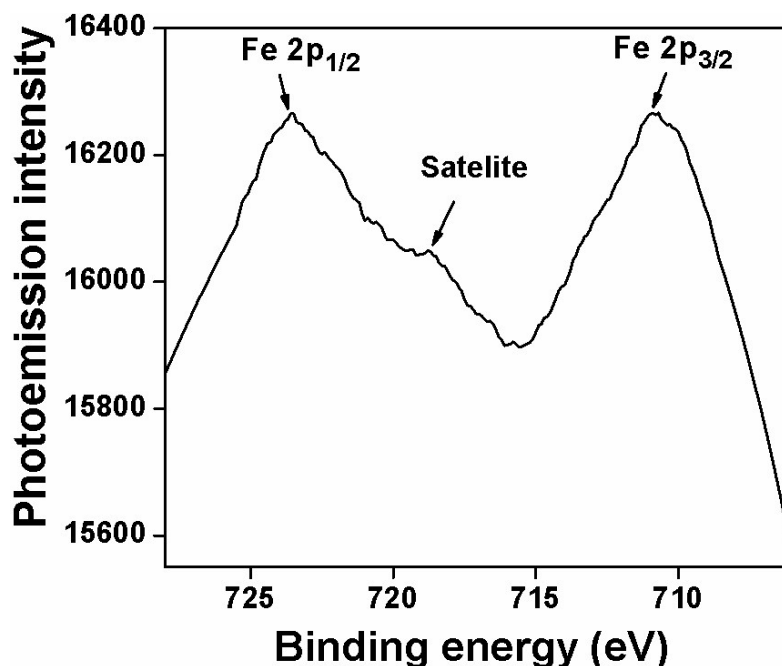
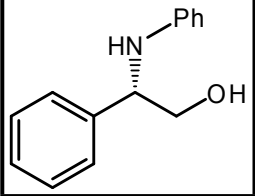
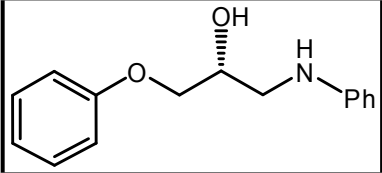
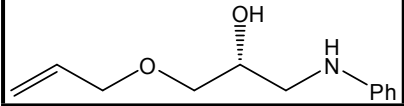


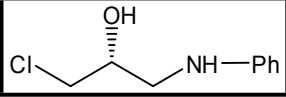
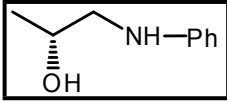
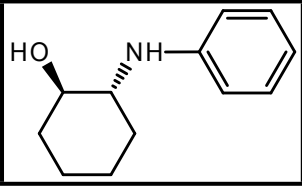
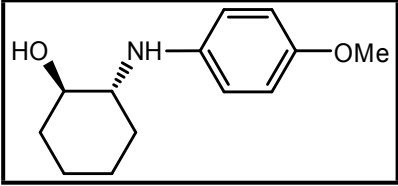
Figure S11. The XPS spectrum of the reused Fe@SBSAL catalyst.

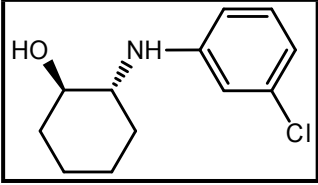
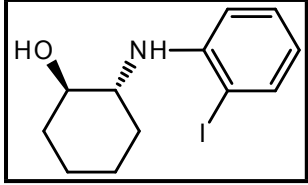
The electron paramagnetic resonance (EPR) spectrum of Fe@SBSAL exhibited the +3 oxidation state of grafted iron species as shown in Figure S6. In order to investigate the elemental composition and oxidation state of the reused catalyst the X-ray photoelectron spectroscopic (XPS) analysis has been carried out. Figure S11 represents the high resolution spectra of Fe_{2p} demonstrating the peak at 710.8 eV due to Fe 2p_{3/2} and another binding energy peak appearing at 723.5 eV, which is attributed to the presence of Fe 2p_{1/2}. To identify the dominating oxidation state of iron (+3 or +2) the relative position of the satellite peak (weak) is analyzed here. Owing to the similarity of results obtained from many research experiments,⁸ the presence of satellite peak at 718.9 eV and the binding energy difference of 8.1 eV suggested the existence of Fe⁺³ oxidation state in the reused catalyst. Thus, XPS analysis result revealed that the oxidation state of Fe(III) in Fe@SBSAL after the catalytic reaction has been retained.

Section-S2

¹H NMR and HPLC data of isolated pure products

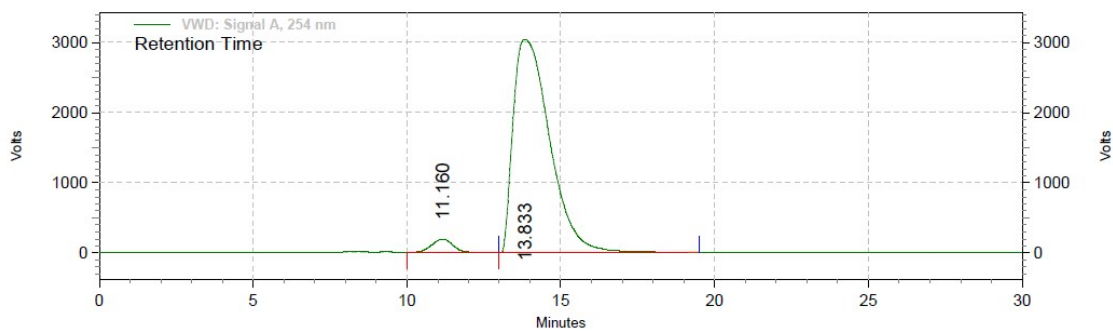
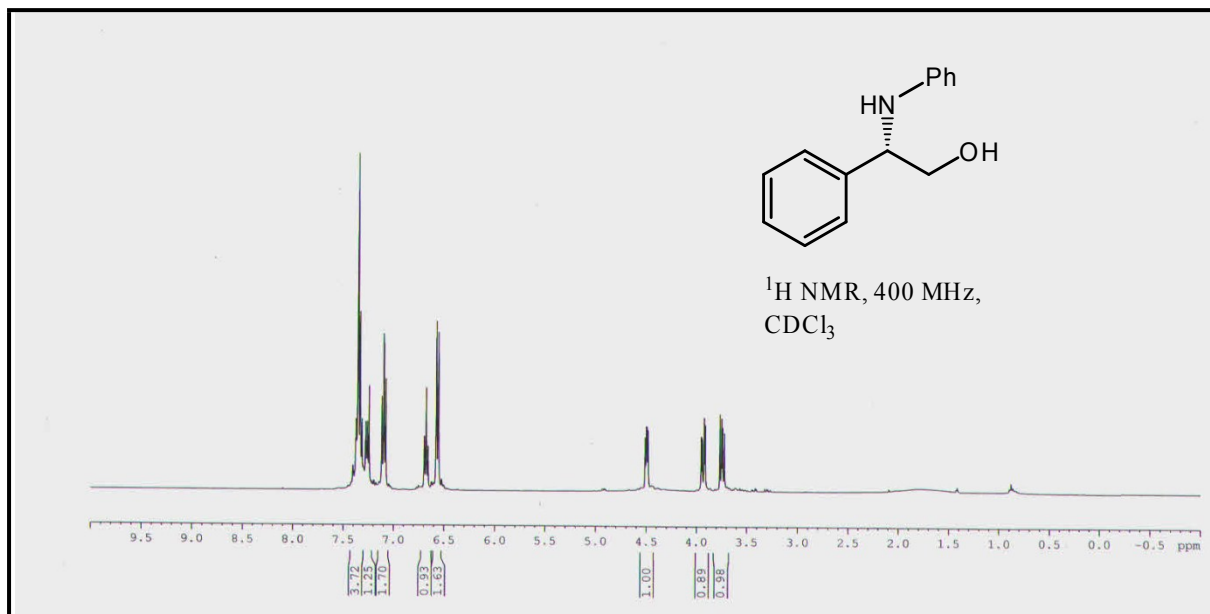
 <p>The structure shows a benzene ring attached to a chiral carbon atom. This carbon is also bonded to a hydrogen atom (dashed bond) and a hydroxymethyl group (-CH₂OH). The adjacent carbon is bonded to a phenyl group (-NHPh).</p>	<p>The compound was isolated by column chromatography (hexane/AcOEt 90/10) as a light yellow liquid.; $[\alpha]_{\text{D}}^{27} = +30.0$ ($c = 0.5$, CHCl_3); The ee 96% on HPLC (Chiralpak OD column) mobile phase, 90/10 hexane/<i>i</i>-PrOH; flow rate 1 ml/min, retention time. : 11.16 min (minor), 13.83 min. (major); ¹H NMR (400MHz, CDCl_3): $\delta = 3.72\text{-}3.76$ (m, 1H), 3.91-3.95 (dd, $J = 4.4$ and 6.8 Hz, 1H), 4.48-4.51 (m, 1H), 6.56 (d, $J = 7.6$ Hz, 2H), 6.67 (t, 1H), 7.12-7.09 (t, 2H), 7.12-7.40 (m, 5H) ppm.</p>
 <p>The structure shows a benzene ring attached to an oxygen atom, which is part of a benzyloxy group (-OCH₂CH₂-). This is followed by a chiral carbon atom bonded to a hydroxyl group (-OH, dashed bond) and a hydrogen atom (wedged bond). The adjacent carbon is bonded to a phenyl group (-NHPh).</p>	<p>The compound was isolated by column chromatography (hexane/AcOEt 90/10) as a light yellow liquid.; $[\alpha]_{\text{D}}^{27} = -33.5$ ($c = 0.5$, CHCl_3); The ee 99% on HPLC (Chiralpak OD column) mobile phase, 90/10 hexane/<i>i</i>-PrOH; flow rate 1 ml/min, retention time. : 10.76 min (minor), 14.71 min. (major); ¹H NMR (400 MHz, CDCl_3): $\delta = 3.14\text{-}3.19$ (m, 1H), 3.19-3.33 (m, 1H), 4.91-4.96 (m, 2H), 4.12-4.15 (m, 1H), 6.57 (d, $J = 8.4$ Hz, 2H), 6.65 (t, 1H), 6.82 (d, $J = 8.4$ Hz, 2H), 6.88 (t, 1H), 7.07-7.13 (m, 2H), 7.18-7.22 (m, 2H) ppm.</p>
 <p>The structure shows an allyloxy group (-OCH₂CH₂CH=CH₂) attached to a chiral carbon atom. This carbon is also bonded to a hydroxyl group (-OH, dashed bond) and a hydrogen atom (wedged bond). The adjacent carbon is bonded to a phenyl group (-NHPh).</p>	<p>The compound was isolated by column chromatography (hexane/AcOEt 90/10) as a yellow liquid.; $[\alpha]_{\text{D}}^{27} = -37.8$ ($c = 1.5$, CHCl_3); The ee 97% on HPLC (Chiralpak OD column) mobile phase, 90/10 hexane/<i>i</i>-PrOH; flow rate 1 ml/min, retention time. : 11.62 min (major), 16.66 min. (minor) ¹H NMR (400 MHz, CDCl_3): $\delta = 2.60$ (s, br, 1H), 3.08 (dd, $J = 5.6, 7.2$ Hz, 1H), 3.23 (dd, $J = 4.4, 8.8$ Hz, 1H), 3.40- 3.44 (m, 1H), 3.48 (dd, $J = 4, 5.6$ Hz, 1H), 3.93-3.98 (m, 3H), 5.12-5.24 (m, 1H), 5.79-5.87 (m, 1H), 6.56-6.66 (m, 3H), 7.08-7.12 (m, 2H) ppm.</p>

	<p>The compound was isolated by column chromatography (hexane/AcOEt 90/10) as a light yellow liquid.; $[\alpha]^{27}_D = -30.1$ ($c = 1.0$, CHCl_3); The ee 99% on HPLC (Chiralpak OD column) mobile phase, 90/10 hexane/<i>i</i>-PrOH; flow rate 1 ml/min, retention time. : 16.69 min (minor), 18.14 min. (major) ; $^1\text{H NMR}$ (400 MHz, CDCl_3): δ 2.98 (s, br, 1H), 3.13 (dd, $J=6.4, 7.2$ Hz, 1H), 3.29 (dd, $J=4.4, 9.2$ Hz, 1H), 3.49-3.61 (m, 2H), 3.96-4.02 (m, 1H), 6.58-6.62 (m, 2H), 6.68-6.72 (m, 1H), 7.08-7.17 (m, 2H).</p>
	<p>The compound was isolated by column chromatography (hexane/AcOEt 92/8) as a light yellow liquid.; $[\alpha]^{27}_D = -28.6$ ($c = 1.0$, CHCl_3); The ee 83% on HPLC (Chiralpak OD column) mobile phase, 90/10 hexane/<i>i</i>-PrOH; flow rate 1 ml/min, retention time. : 12.27 min (major), 15.13 min. (minor) ; $^1\text{H NMR}$ (400 MHz, CDCl_3): δ 1.22 (d, $J = 6.8$ Hz, 3H), 2.94 (dd, $J=4.4, 8.8$ Hz, 1H), 3.17 (dd, $J=3.2, 9.6$ Hz, 1H), 3.94-3.99 (m, 1H), 6.60-6.64 (m, 2H), 6.71 (t, 1H), 7.14-7.19 (m, 2 H).</p>
	<p>The compound was isolated by column chromatography (hexane/AcOEt 90/10) as a white solid.; $[\alpha]^{27}_D = -34.9$ ($c = 0.5$, CHCl_3); The ee 99% on HPLC (Chiralpak OD column) mobile phase, 90/10 hexane/<i>i</i>-PrOH; flow rate 1 ml/min, retention time. (<i>1S,2S</i>): 8.61 min (minor), (<i>1R,2R</i>): 10.47 min. (major) ; $^1\text{H NMR}$ (400 MHz, CDCl_3): δ 1.18–1.24 (m, 1H), 1.25–1.36 (m, 3H), 1.62–1.96 (m, 3H), 2.02–2.04 (m, 2H), 2.91 (br s, 1H), 3.02-3.08 (m, 1H), 3.23-3.28 (m, 1H), 6.62–6.68 (m, 3H), 7.10 (t, 2H), ppm</p>
	<p>The compound was isolated by column chromatography (hexane/AcOEt 92/8) as a white solid.; $[\alpha]^{27}_D = -25.8$ ($c = 0.8$, CHCl_3); The ee 97% on HPLC (Chiralpak OD column) mobile phase, 90/10 hexane/<i>i</i>-PrOH; flow rate 1 ml/min,</p>

	<p>retention time. (<i>1S,2S</i>): 9.28 min (minor), (<i>1R,2R</i>): 13.92 min. (major) ; ¹H NMR (400 MHz, CDCl₃): δ 1.30–1.42 (m, 4H), 1.68–1.77 (m, 2H), 2.04–2.13 (m, 2H), 2.84 (br s, 1H), 2.96–3.02 (m, 1H), 3.29–3.35 (m, 1H), 3.74 (s, 3H), 6.66–6.70 (m, 2H), 6.75–6.79 (m, 2H), ppm</p>
	<p>The compound was isolated by column chromatography (hexane/AcOEt 90/10) as a yellow liquid; $[\alpha]_D^{27} = -28.3$ (c = 0.5, CHCl₃); The ee 98% on HPLC (Chiralpak OD column) mobile phase, 90/10 hexane/<i>i</i>-PrOH; flow rate 1 ml/min, retention time. (<i>1S,2S</i>): 9.67 min (minor), (<i>1R,2R</i>): 11.78 min. (major) ; ¹H NMR (400 MHz, CDCl₃): δ 1.10–1.14 (m, 1H), 1.23–1.44 (m, 3H), 1.50–1.59 (m, 1H), 1.73–1.80 (m, 1H), 2.08–2.13 (m, 2H), 3.08–3.14 (m, 1H), 3.35–3.41 (m, 1H), 3.74 (s, 3H), 6.69–6.61 (dd, <i>J</i>=1.2, 2.8 Hz, 1H), 6.71–6.72 (m, 2H), 7.08 (t, 1H) ppm.</p>
	<p>The compound was isolated by column chromatography (hexane/AcOEt 93/7) as a yellow liquid; $[\alpha]_D^{27} = -29.0$ (c = 1.0, CHCl₃); The ee 98% on HPLC (Chiralpak OD column) mobile phase, 90/10 hexane/<i>i</i>-PrOH; flow rate 1 ml/min, retention time. (<i>1S,2S</i>): 3.67 min (minor), (<i>1R,2R</i>): 5.28 min. (major) ; ¹H NMR (400 MHz, CDCl₃): δ 0.81–0.88 (m, 1H), 1.07–1.50 (m, 4H), 1.65–1.99 (m, 1H), 2.01–2.08 (m, 2H), 3.13 (br s, 1H), 3.38–3.44 (m, 1H), 3.67–3.84 (m, 1H), 6.38–6.42 (m, 1H), 6.70 (d, <i>J</i>=8 Hz, 1H), 7.10–7.15 (m, 1H), 7.58–7.61 (m, 1H) ppm.</p>

Section-S3

(S)-2-phenyl-2-(phenylamino)ethanol (Table 2, entry 1)

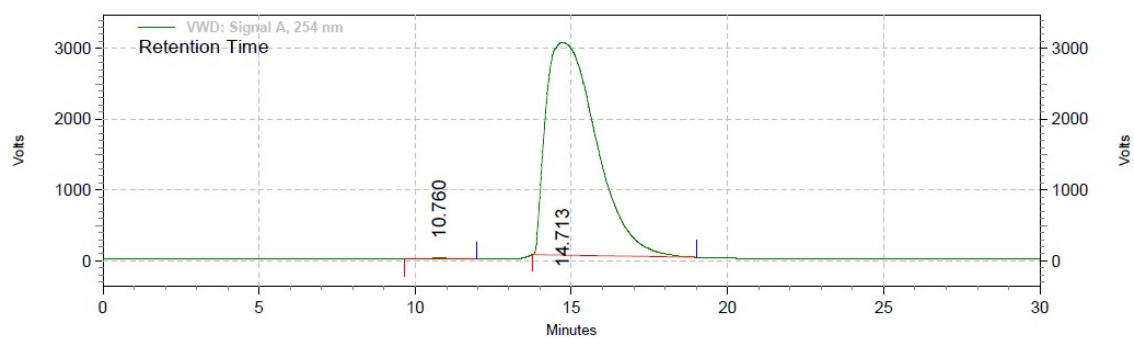
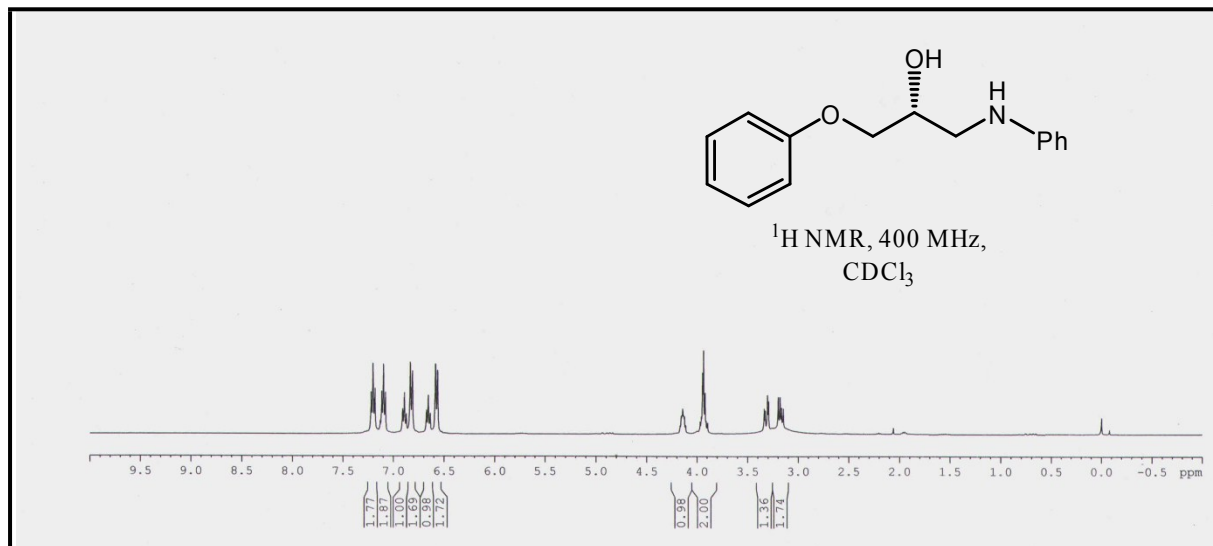


VWD: Signal A, 254 nm Results

Retention Time	Area	Area %	Height	Height %
11.160	159040667	3.63	3267300	6.01
13.833	4217380446	96.37	51069369	93.99

Totals	4376421113	100.00	54336669	100.00
--------	------------	--------	----------	--------

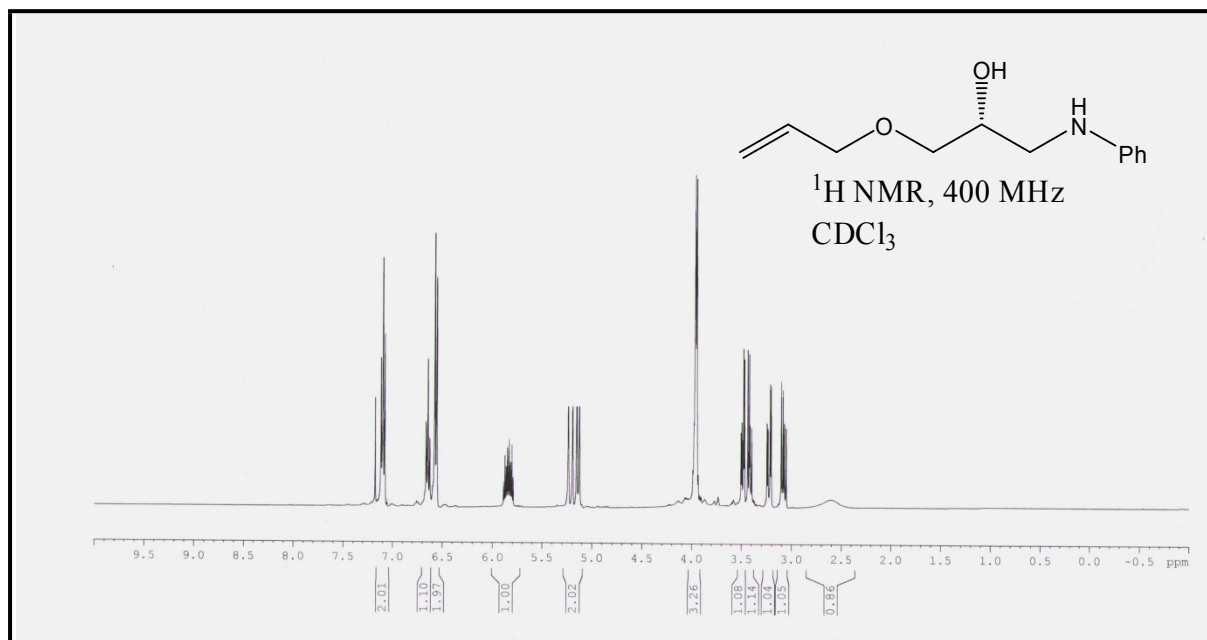
(R)-1-phenoxy-3-(phenylamino)propan-2-ol (Table 2, entry 2)



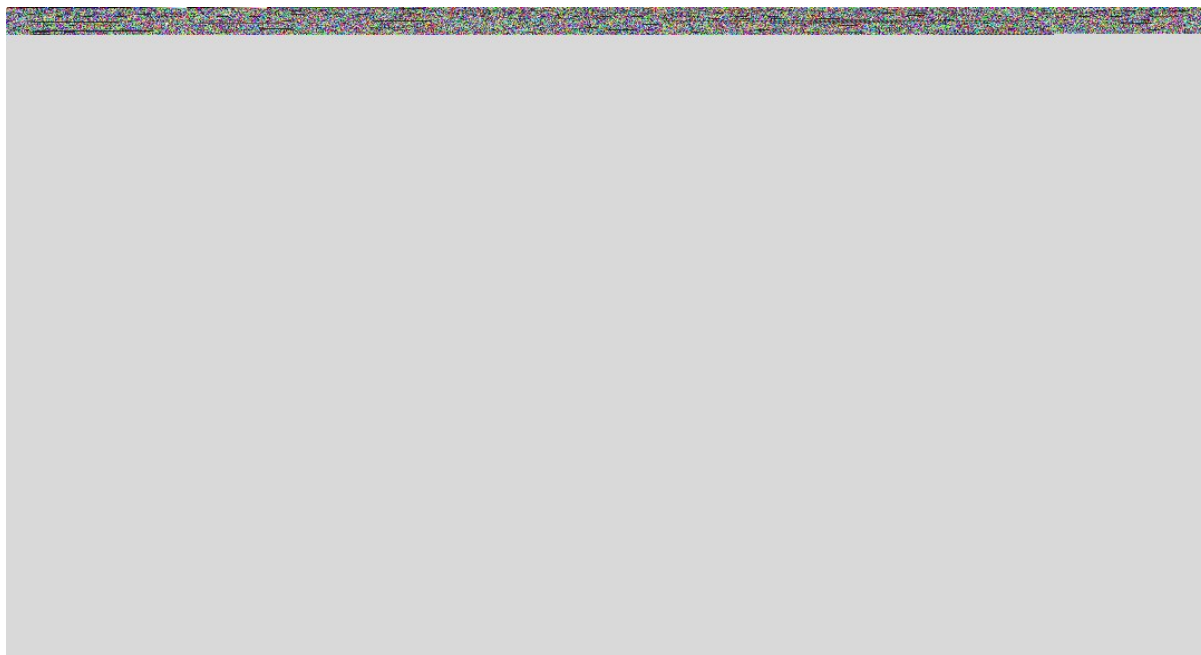
**VWD: Signal A,
254 nm Results**

Retention Time	Area	Area %	Height	Height %
10.760	12868816	0.23	334312	0.66
14.713	5650121242	99.77	50454649	99.34
Totals	5662990058	100.00	50788961	100.00

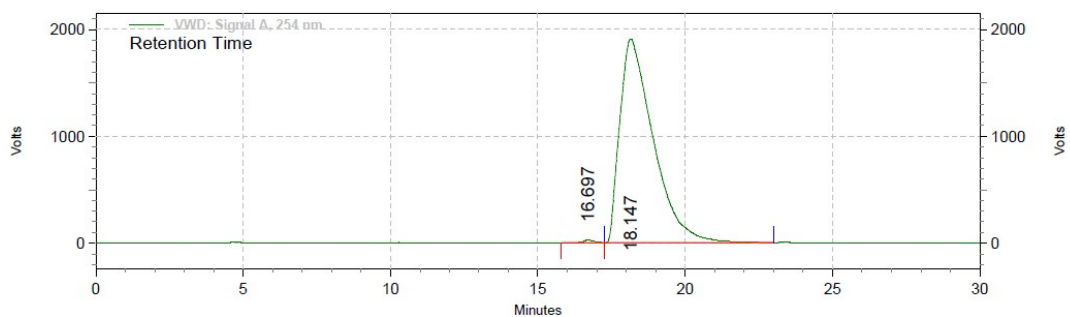
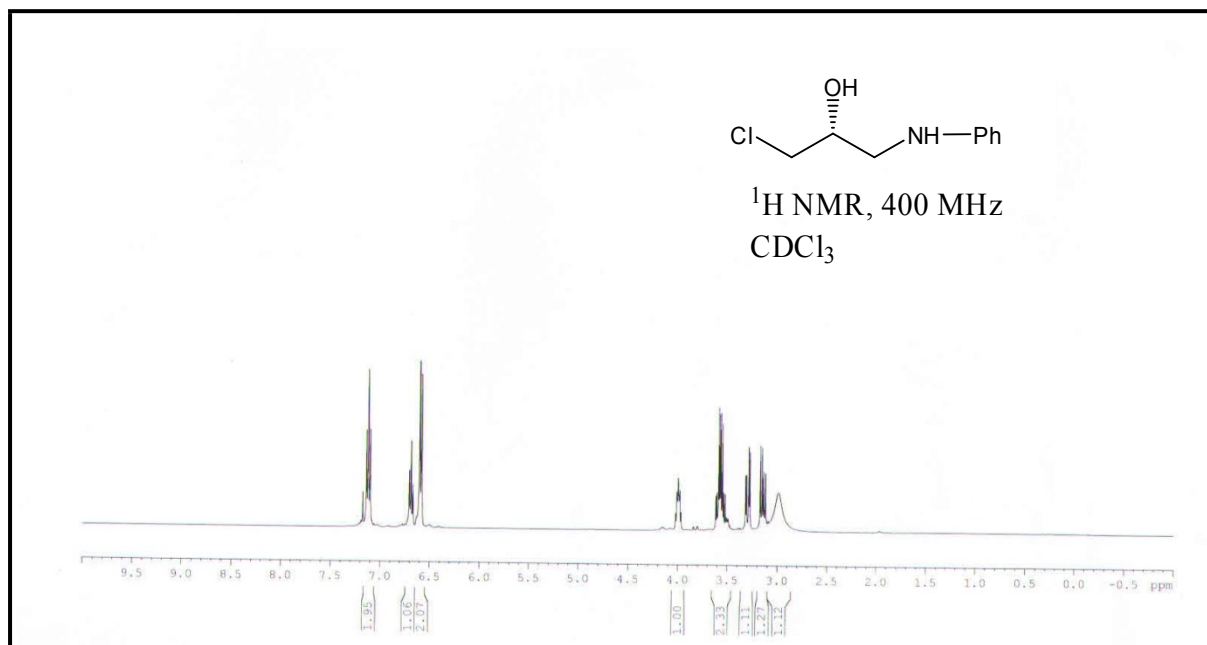
(R)-1-(allyloxy)-3-(phenylamino)propan-2-ol (Table 2, entry 3)



CC



(R)-1-chloro-3-(phenylamino)propan-2-ol (Table 2, entry 4)

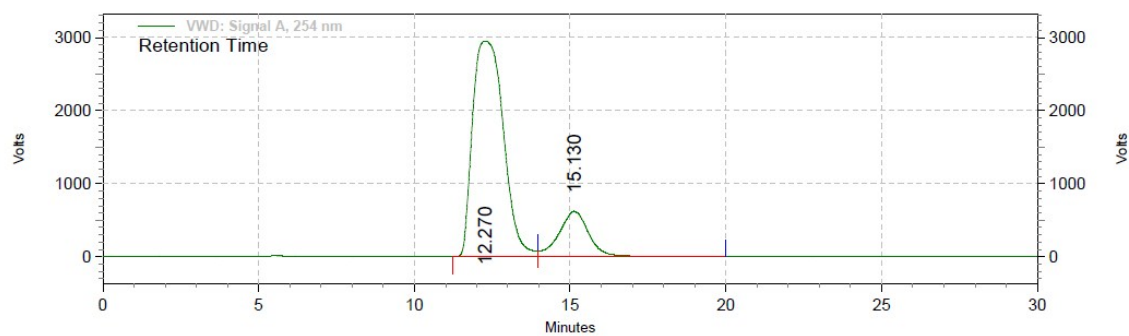
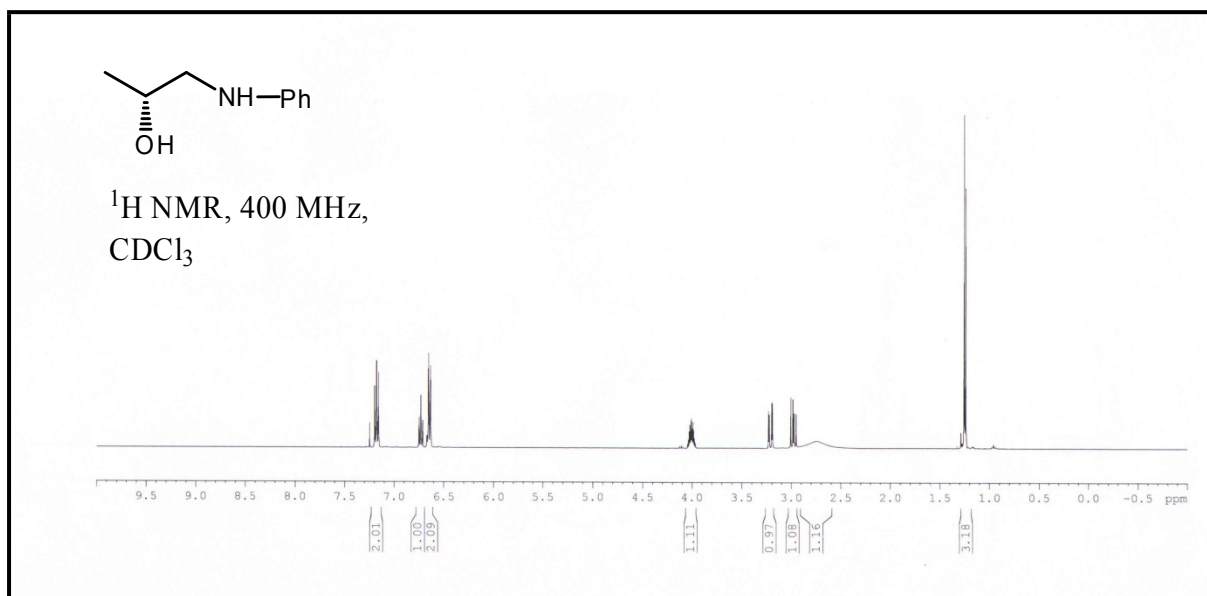


**VWD: Signal A,
254 nm Results**

Retention Time	Area	Area %	Height	Height %
16.697	12712378	0.50	451924	1.39
18.147	2526551422	99.50	32043382	98.61

Totals	2539263800	100.00	32495306	100.00
--------	------------	--------	----------	--------

(R)-1-(phenylamino)propan-2-ol (Table 2, entry 5)

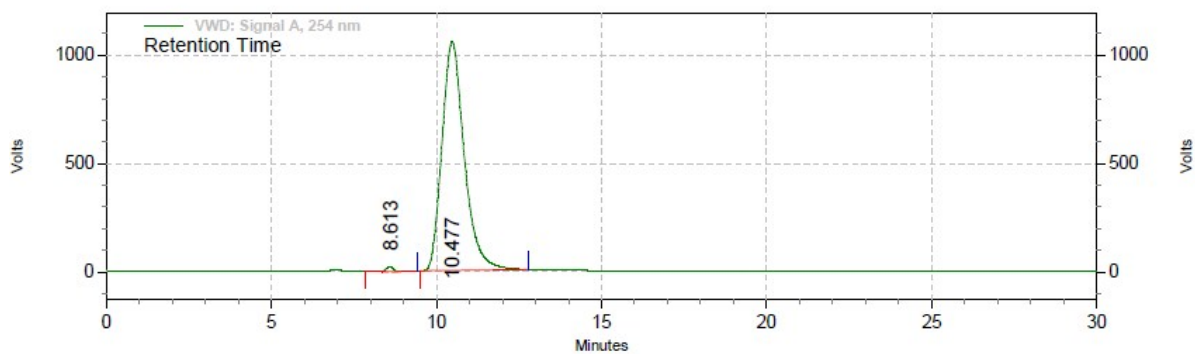
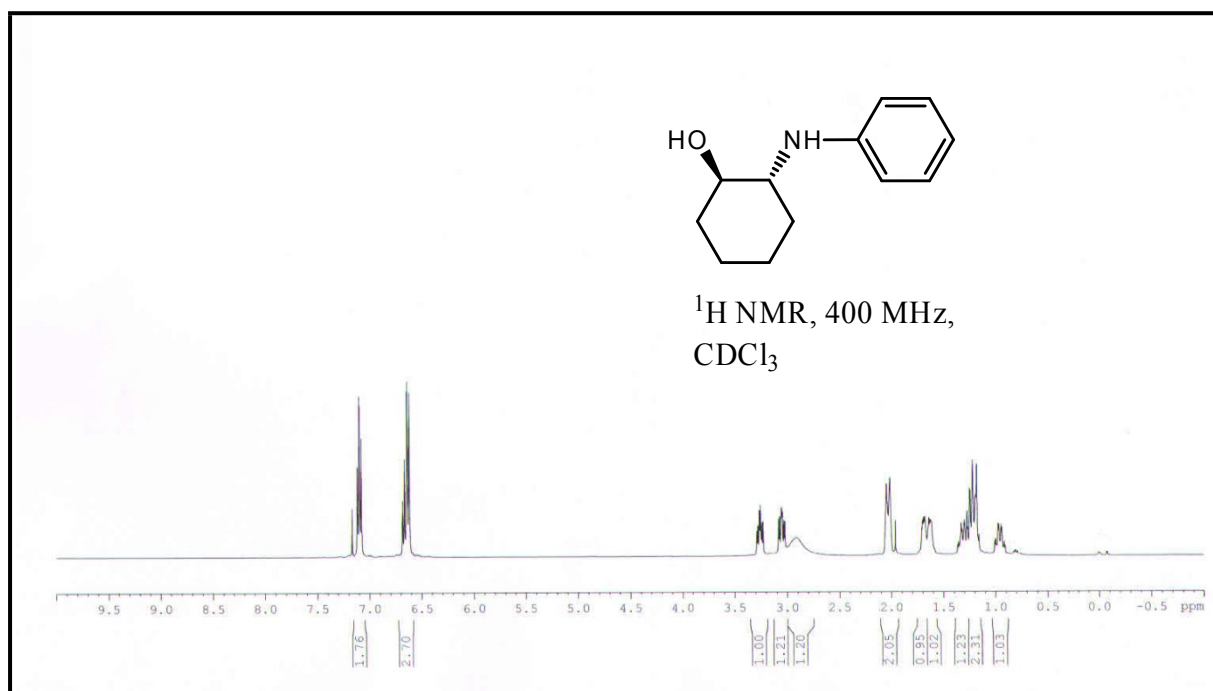


**VWD: Signal A,
254 nm Results**

Retention Time	Area	Area %	Height	Height %
12.270	3409429251	82.99	49538435	82.62
15.130	698675006	17.01	10418040	17.38

Totals	4108104257	100.00	59956475	100.00
--------	------------	--------	----------	--------

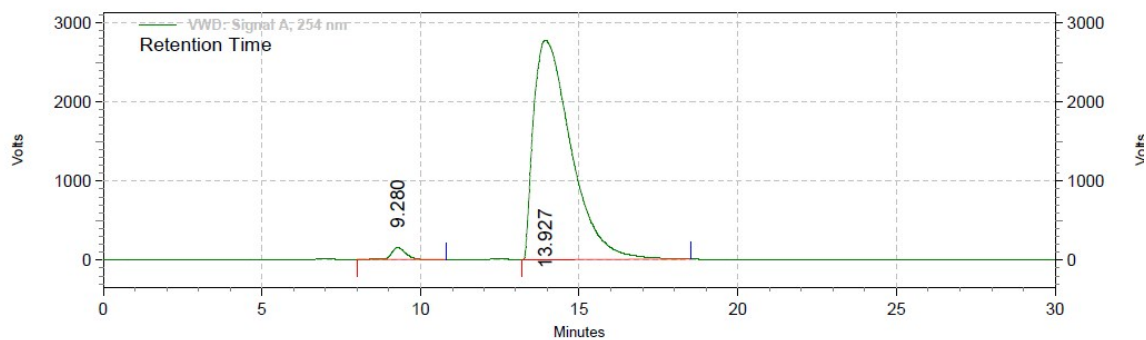
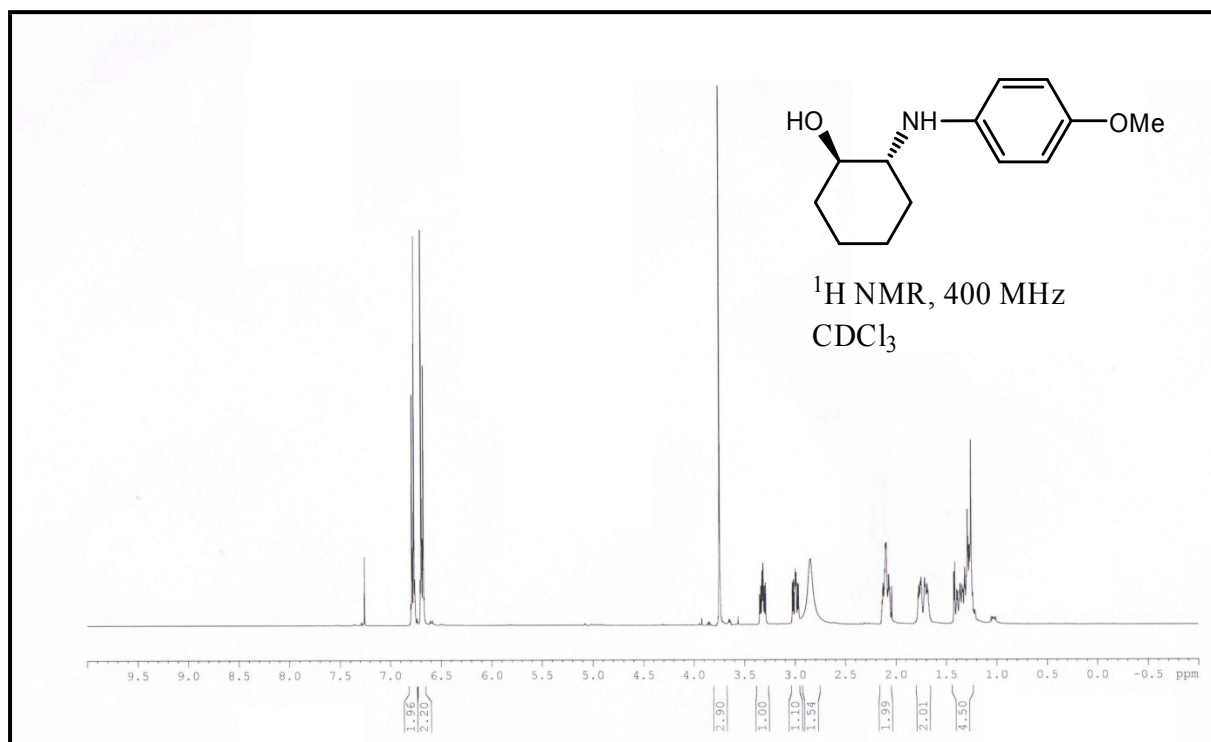
(1R,2R)-2-(phenylamino)cyclohexanol (Table 2, entry 6)



**VWD: Signal A,
254 nm Results**

Retention Time	Area	Area %	Height	Height %
8.613	352282	0.04	7605	0.04
10.477	833734225	99.96	17729310	99.96
Totals	834086507	100.00	17736915	100.00

(1R,2R)-2-(4-methoxyphenylamino)cyclohexanol (Table 2, entry 7)

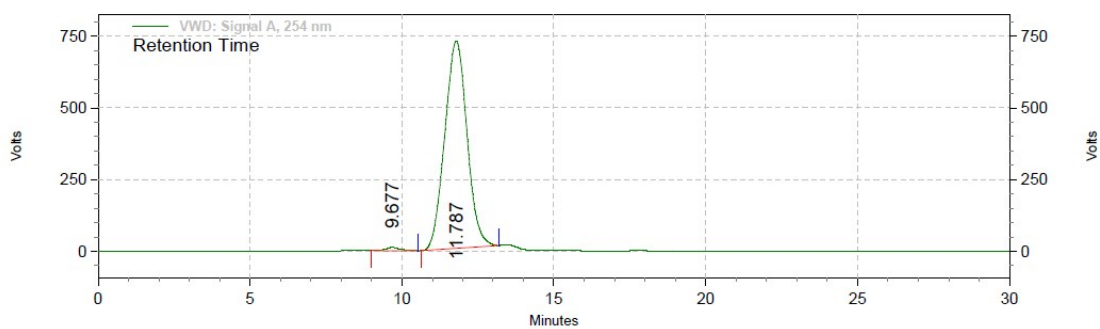
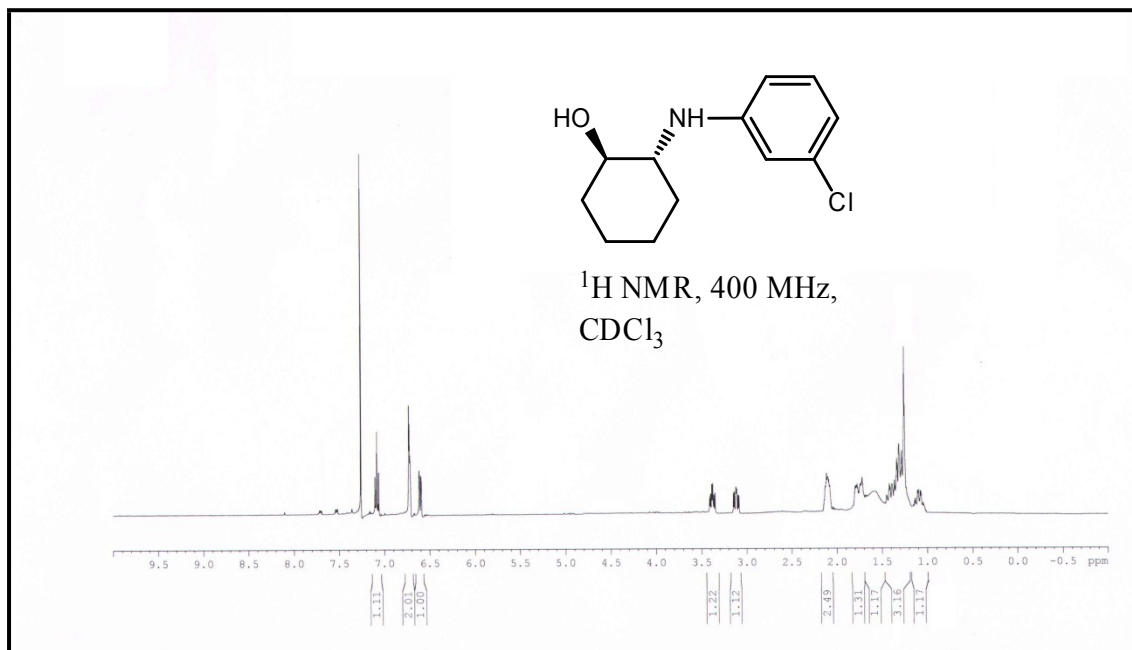


**VWD: Signal A,
 254 nm Results**

Retention Time	Area	Area %	Height	Height %
9.280	80058133	2.05	2575270	5.23
13.927	3825527564	97.95	46632179	94.77

Totals	3905585697	100.00	49207449	100.00
--------	------------	--------	----------	--------

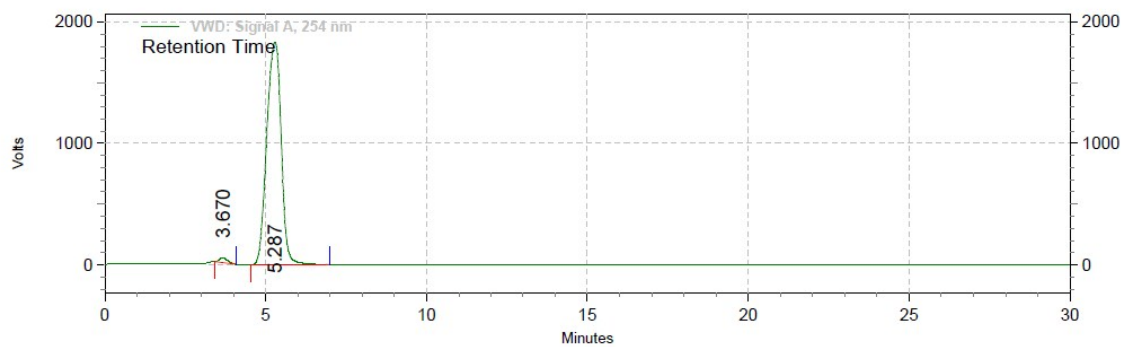
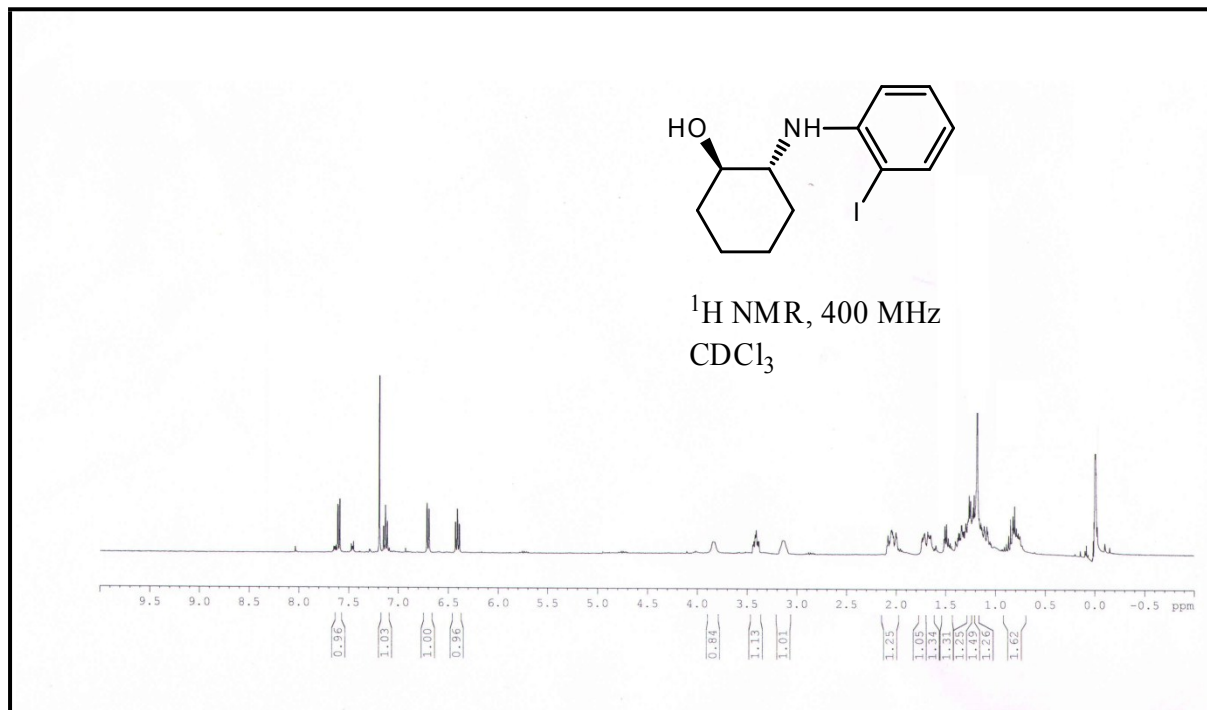
(1R,2R)-2-(3-chlorophenylamino)cyclohexanol (Table 2, entry 8)



**VWD: Signal A,
254 nm Results**

Retention Time	Area	Area %	Height	Height %
9.677	6361751	1.02	182160	1.48
11.787	617604314	98.98	12146791	98.52
Totals	623966065	100.00	12328951	100.00

(1R,2R)-2-(2-iodophenylamino)cyclohexanol (Table 2, entry 9)



**VWD: Signal A,
254 nm Results**

Retention Time	Area	Area %	Height	Height %
3.670	12066186	1.24	686123	2.18
5.287	959933882	98.76	30792818	97.82
Totals	972000068	100.00	31478941	100.00

Section-S4

References:

1. L. Canali, E. Cowan, H. Deleuze, C.L. Gibson and D.C. Sherrington, *J. Chem. Soc. Perkin Trans.*, 2000, **1**, 2055
2. K. Yu, Z. Gu, R. Ji, L. L. Lou, F. Ding, C. Zhanga and S. Liu, *Journal of Catalysis*, 2007, **252** 312–320.
3. S. Roy, T. Chatterjee, M. Pramanik, A. Bhaumik and S. M. Islam, *J. Mol. Catal. A: Chemical*, 2014, **386**, 78
4. R. I. Kureshy, K. J. Prathap, M. Kumar, P. K. Bera, N. H. Khan, S. H. R. Abdi and H. C. Bajaj, *Tetrahedron*, 2011, **67**, 8300-8307.
5. M. Kumar, R. I. Kureshy, S. Saravanan, S. Verma, A. Jakhar, N. H. Khan, S. H. R. Abdi, and H. C. Bajaj, *Org. Lett.*, 2014, **16**, 2798-2801.
6. J. Sun, Z. Dai, M. Yang, X. Pan and C. Zhu, *Synthesis* 2008, **13**, 2100-2104.
7. K. Sarkar, K. Dhara, M. Nandi, P. Roy, A. Bhaumik and P. Banerjee, *Adv. Funct. Mater.* 2009, **19**, 223-234.
8. (a) T. Yamashita and P. Hayes, *Appl. Surf. Sci.*, 2008, **254**, 2441-2449; (b) A. A. Makarova, E. V. Grachova, V. S. Neudachina, L. V. Yashina, A. Bluher, S. L. Molodtsov, M. Mertig, H. Ehrlich, V. K. Adamchuk, C. Laubschat, D. V. Vyalikh, *Scientific Reports*, 2015, DOI: 10.1038/srep08710; (c) M. M. Vadiyar, S. C. Bhise, S. K. Patil, S. A. Patil, D. K. Pawar, A. V. Ghule, P. S. Patil and S. S. Kolekar, *RSC Adv.*, 2015, **5**, 45935-45942.